Observation of the Berezinskii-Kosterlitz-Thouless Transition in a Two-Dimensional Bose Gas via Matter-Wave Interferometry

S. Sunami,[1,*] V. P. Singh,[2,3] D. Garrick,[1] A. Beregi,[1] A. J. Barker,[1] K. Luksch,[1] E. Bentine,[1] L. Mathey,[3,4] and C. J. Foot[1]

[1]*Clarendon Laboratory, University of Oxford, Oxford OX1 3PU, United Kingdom*
[2]*Institut für Theoretische Physik, Leibniz Universität Hannover, Appelstraße 2, 30167 Hannover, Germany*
[3]*Zentrum für Optische Quantentechnologien and Institut für Laserphysik, Universität Hamburg, 22761 Hamburg, Germany*
[4]*The Hamburg Centre for Ultrafast Imaging, Luruper Chaussee 149, Hamburg 22761, Germany*

(Received 20 August 2021; revised 15 December 2021; accepted 18 April 2022; published 22 June 2022)

We probe local phase fluctuations of trapped two-dimensional Bose gases using matter-wave interferometry. This enables us to measure the phase correlation function, which changes from an algebraic to an exponential decay when the system crosses the Berezinskii-Kosterlitz-Thouless (BKT) transition. We determine the temperature dependence of the BKT exponent η and find the critical value $\eta_c = 0.17(3)$ for our trapped system. Furthermore, we measure the local vortex density as a function of the local phase-space density, which shows a scale-invariant behavior across the transition. Our experimental investigation is supported by Monte Carlo simulations and provides a comprehensive understanding of the BKT transition in a trapped system.

DOI: 10.1103/PhysRevLett.128.250402

One of the most intriguing phase transitions is the Berezinskii-Kosterlitz-Thouless (BKT) transition, which lies within the *XY* universality class [1,2]. Two-dimensional (2D) systems in this universality class display quasi-long-range order at nonzero temperatures below the transition, whereas true long-range order is precluded by thermal fluctuations [3,4]. Above the transition, the system forms a disordered state. This transition is characterized by the first-order correlation function $g_1(\boldsymbol{r},\boldsymbol{r}') = \langle\Psi^\dagger(\boldsymbol{r})\Psi(\boldsymbol{r}')\rangle$, where $\Psi(\boldsymbol{r})$ is the bosonic field operator at location $\boldsymbol{r}$, which changes from algebraic scaling $\sim r^{-\eta}$ in the superfluid phase, to exponential scaling in the thermal phase, with universal exponent $\eta_{\mathrm{BKT}} = 0.25$ at the transition. The origin of this change is the BKT mechanism, which consists of the unbinding of vortex–antivortex pairs at the phase transition, underscoring the topological nature of the transition. The unbound vortices are strong phase defects and suppress the quasi-long-range order. The BKT transition occurs in a wide range of physical systems such as liquid helium [5], superconducting films [6], Josephson junction arrays [7], ultracold atoms [8], and polariton condensates [9].

Ultracold atoms have enabled detailed studies of the BKT transition. These systems have a wide range of trappable quantum liquids, that have tunable interactions and consist of bosonic or fermionic particles. This has led to the observation of coherence and superfluid properties [8,10–15], universal scaling behavior [16], and thermally activated vortices [8,17]. The BKT transition in a harmonically trapped 2D quantum gas was studied via matter-wave interferometry [8] and via measurement of the momentum distribution [18,19]. The microscopic description of order in such an inhomogeneous system typically invokes the local density approximation (LDA), which relates the observed phenomenon to the universal description of a uniform system. The LDA is essential for the understanding of scale-invariant and superfluid properties of inhomogeneous 2D systems [10,16]. Reference [20] suggested that the LDA can also be used to describe the correlation properties of an inhomogeneous 2D gas, which was not applied in previous measurements where only integrated quantities were measured. This resulted in saturation of the exponent at low temperatures [8] as well as a critical exponent 5 times larger than that predicted for η_{BKT} [18]. To disentangle the spatial inhomogeneity of the system and the universality of the BKT transition in ultracold atomic systems, it is crucial to access the local fluctuations of the system, rather than global or integrated observables.

In this Letter, we report the direct observation of local phase fluctuations by a selective probing of the relative phase between a pair of 2D Bose gases. We use matter-wave homodyning and selectively image a slice of the interference pattern [21] to access *local* phase fluctuations. This critical improvement allows direct measurement of the phase correlation function and the local vortex density, which are essential to characterize the BKT transition, as we demonstrate in this Letter. We identify the critical temperature of the BKT transition by a change in the functional form of the correlation function, which results in a measured value of critical exponent $\eta_c = 0.17(3)$ for our trapped system. We examine the temperature dependence of the thermally created vortices, which proliferates above the critical temperature and exhibits a scale-invariant

behavior. We benchmark these experimental measurements by carrying out Monte Carlo (MC) simulations.

Our experimental apparatus is described in detail in Refs. [21,22]. A cloud of approximately 7×10^4 ^{87}Rb atoms is confined in a cylindrically symmetric 2D potential, with weak trap frequencies of $\omega_r/2\pi = 11$ Hz in the horizontal plane and a double-well potential in the vertical direction z. The double well has vertical trap frequencies of $\omega_z/2\pi = 1$ kHz for each potential minimum and each well confines $N \approx 3.5 \times 10^4$ atoms. For the range of temperatures and atom numbers in this work, the quasi-2D conditions $\hbar\omega_z > k_B T$ and $\hbar\omega_z > \mu$ are satisfied, where $\hbar$ is the reduced Planck constant, k_B the Boltzmann constant, T is the temperature of the cloud, and μ is the chemical potential. The characteristic dimensionless 2D interaction strength is $\tilde{g} = \sqrt{8\pi} a_s/\ell_0 = 0.076$, where a_s is the 3D scattering length and $\ell_0 = \sqrt{\hbar/(m\omega_z)}$ is the harmonic oscillator length along z for an atom of mass m. After loading into the double well, the gas is held for 500 ms to allow equilibration [8]. The final temperature of the gas is in the range 31–47 nK, which is controlled by forced evaporation. We set the temperature scale for our system using the condensation temperature of an ideal 2D Bose gas in a harmonic trap, $T_0 = \sqrt{6N}(\hbar\omega_r/\pi k_B) \approx 75$ nK.

The detection scheme is illustrated in Fig. 1(a). To observe the matter-wave interference, the trap is abruptly turned off, releasing the pair of 2D gases for a time-of-flight (TOF) expansion of duration $t_{\mathrm{TOF}} = 16.2$ ms. Once released, the clouds expand along the z direction [23,24] and an interference pattern along z appears. We image a thin slice of the density distribution with thickness $L_y = 5$ μm, as indicated in Fig. 1(a). The density profile, such as that shown in Fig. 1(b), is obtained by integrating along z and averaging over many images. This profile is a bimodal distribution having a Thomas-Fermi (TF) profile of the quasicondensate and a broad Gaussian of the thermal wings [25], as illustrated in Fig. 1(c). In contrast to the true (3D) condensate, the quasicondensate in two dimensions displays fluctuating phase and supports both thermal and superfluid phases of the BKT transition [25–28]. We determine the quasicondensate fraction (number of atoms within the TF profile divided by the total number of atoms) and show its temperature dependence in Fig. 1(d), along with the MC results [29], which yields the onset of quasicondensation at $T_{\mathrm{qc}}/T_0 \sim 0.7$.

The local fluctuations of the interference fringes contain the phase information of *in situ* clouds. At each location x, we fit the interference pattern with the function [47]

$$\rho_x(z) = \rho_0 \exp(-z^2/2\sigma^2)\{1 + c_0 \cos[kz + \theta(x)]\}, \qquad (1)$$

where $\rho_0, \sigma, c_0, k, \theta(x)$ are fit parameters. The extracted phase $\theta(x)$ encodes a specific realization of the fluctuations of the *in situ* local relative phase between the pair of 2D gases. For each experimental run, we calculate the

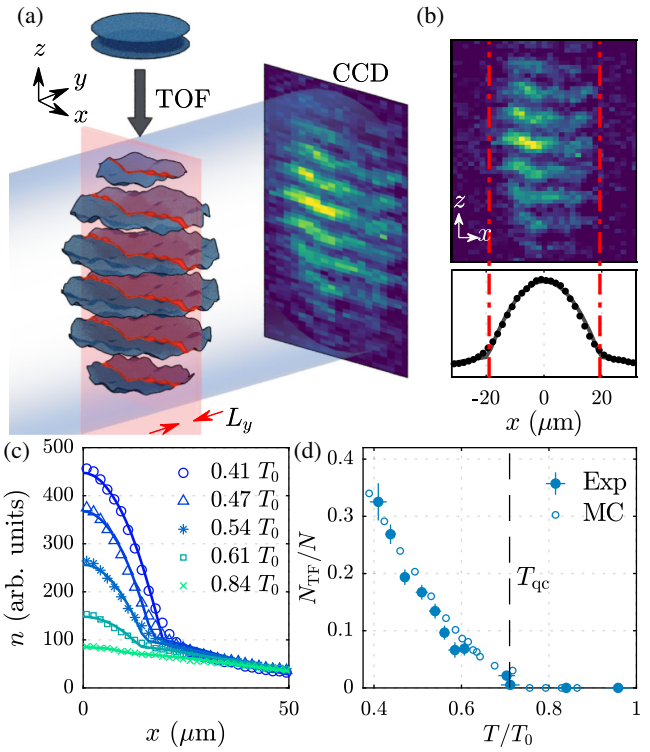

FIG. 1. Probing local phase fluctuations using matter-wave interference. (a) Schematic of the experimental procedure. We begin with quasi-2D Bose gases trapped in a double-well potential (blue discs, top). The clouds fall and undergo time-of-flight expansion, such that they spatially overlap and produce interference fringes with fluctuating phases (blue wavy planes). The red sheet of thickness L_y denotes the thin laser beam that repumps a slice of atoms. We image repumped atoms using resonant light (depicted as a blue beam propagating along the y direction). (b) An example of a single matter-wave interference image (top) and averaged density profile obtained by integrating along z (bottom). The red dash-dotted lines indicate the boundaries of the Thomas-Fermi region of quasicondensate; see text. Gray solid line is the result of bimodal fit. (c) Density profiles at different temperatures, where the continuous lines are bimodal fits; see text. (d) Fraction of atoms in the TF profile of the cloud from the experiment (filled markers) and the Monte Carlo simulation (open markers). The error bars of the experimental results denote standard errors.

two-point phase correlation function $e^{i[\theta(x)-\theta(x')]}$ at locations x and x'. We then determine the averaged correlation function

$$C_{\mathrm{exp}}(x, x') = \frac{1}{N_r} \sum_j e^{i[\theta(x)-\theta(x')]}, \qquad (2)$$

where the index j runs over N_r individual experimental realizations with $N_r = 220$. We analyze the real part of the correlation function $C^r(x, x') = \mathrm{Re}[C_{\mathrm{exp}}(x, x')]$, which is equal to 1 for perfectly correlated pairs of points and 0 for uncorrelated pairs of points. Figures 2(a)–2(c) show

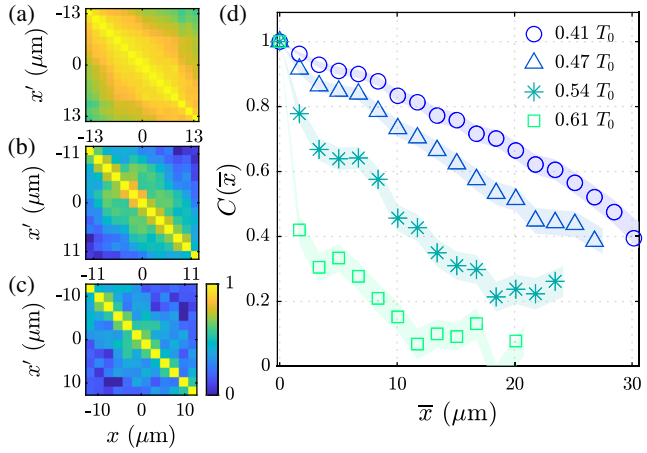

FIG. 2. Correlation properties of 2D Bose gases. (a)–(c) Two-point phase correlation function $C^r(x,x')$, obtained from 220 images, at temperatures of $T/T_0 = 0.41$, 0.51, and 0.59, respectively. (d) Correlation function $C(\bar{x})$ at $T/T_0 = 0.41$, 0.47, 0.54, and 0.61, from top to bottom. The shaded region corresponds to the standard errors and the range of $\bar{x}$ depends on the temperature because of the change of TF diameter; see text.

examples of $C^r(x,x')$, which is related to the one-body correlation function $g_1(\boldsymbol{r},\boldsymbol{r}')$ via [29]

$$C^r(\boldsymbol{r},\boldsymbol{r}') \simeq \frac{\langle \Psi^\dagger(\boldsymbol{r})\Psi(\boldsymbol{r}')\rangle^2}{\langle|\Psi(\boldsymbol{r})|^2\rangle\langle|\Psi(\boldsymbol{r}')|^2\rangle} = \frac{g_1(\boldsymbol{r},\boldsymbol{r}')^2}{n_{2D}^2}, \qquad (3)$$

where n_{2D} is the 2D density. To quantify the decay of correlations, we calculate $C(\bar{x})$ by averaging $C^r(x,x')$ over points with the same spatial separation $\bar{x} = x - x'$ [29]. This averaging was performed over a central region corresponding to 80% of the TF diameter.

The measurements of $C(\bar{x})$ for various temperatures shown in Fig. 2(d) indicate that $C(\bar{x})$ decays slowly at short and intermediate distances for $T/T_0 = 0.41$ and 0.47 but rapidly at increasing distance at higher temperatures of $T/T_0 = 0.54$ and 0.61. This qualitative change of the correlation decay with temperature indicates the crossover to the thermal phase across the BKT transition. $C(\bar{x})$ falls off rapidly at large distances for all temperatures because of the decrease in density towards the boundary of the TF region. This effect of density variation can be incorporated into the BKT picture within the LDA by introducing a spatially varying exponent $\eta_l(\bar{x}) = \eta \max[n(\bar{x})]/n(\bar{x})$ [20,29], where the density contribution $n(\bar{x}) = \langle\sqrt{n(x)n(x+\bar{x})}\rangle$ and η correspond to the averaged value within the TF region.

To characterize the transition point, we fit the correlation function $C(\bar{x})$ with two models: the algebraic model $f_{SF}(\bar{x}) = a\bar{x}^{-2\eta_l(\bar{x})}$, where a and η are the fit parameters, and the exponential model $f_{th}(\bar{x}) = be^{-2\bar{x}/r_0}$, where b and r_0 are the fit parameters. We show the χ^2 values of both fit models in Fig. 3(a). We observe a transition to exponential scaling at $T_c/T_0 = 0.53(1)$; below T_c, f_{SF} is favored, while above T_c, f_{th} better describes the correlation decay having more than a factor of 2 higher p values [29].

The value of T_c increases when the analysis is limited to narrower regions with higher mean density [29] and we expect $T_{c,\mathrm{center}}/T_0 = 0.68(4)$ in the limit of a small analysis region using the MC results. This is close to the theoretical prediction of the critical temperature for harmonically trapped quasi-2D Bose gases within LDA,

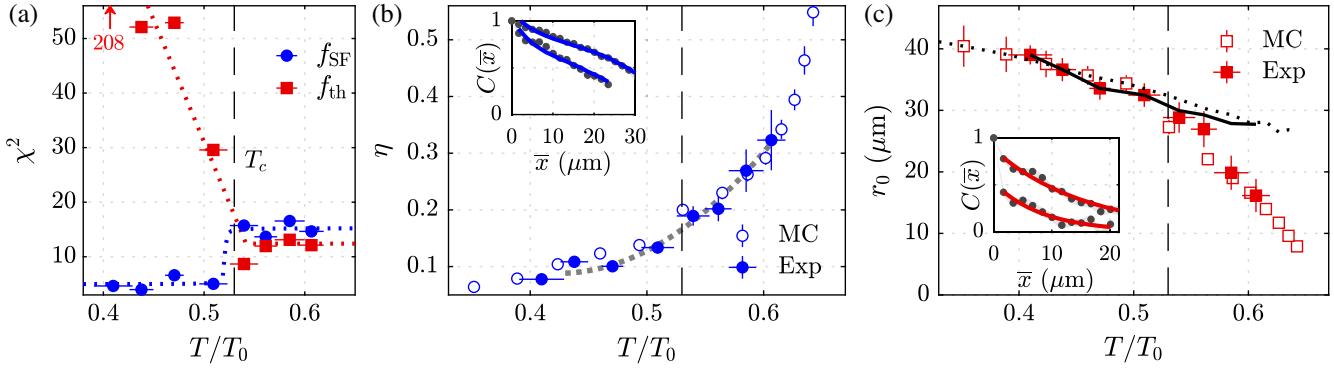

FIG. 3. Characterizing the BKT transition in a 2D Bose gas. (a) χ^2 values of the algebraic fit f_{SF} (blue circles) and exponential fit f_{th} (red squares) for various values of the temperature T/T_0. The dotted lines are the heuristic fits to the temperature dependence of χ^2 to identify the critical point, with arctangent (blue) and a piecewise linear function (red) [29]. The obtained critical temperature $T_c/T_0 = 0.53(1)$ is indicated by the vertical dashed line. (b) Measurements of the algebraic exponent η (filled circles) are compared with the results of Monte Carlo simulations (open circles). η is determined by fitting the correlation function with an algebraic model f_{SF}. The gray dotted line is the quadratic fit to the experimental data used to obtain η_c. The inset shows fitted data in the superfluid regime, at $T/T_0 = 0.41$ and 0.51. (c) Measurements of the correlation length r_0 (filled squares) and the simulation results (open squares), where r_0 is determined by fitting the correlation function with an exponential model f_{th}. The values of the temperature-dependent Thomas-Fermi diameter are shown for the experiment (continuous line) and the simulation (dotted line). The inset shows fitted data in the thermal regime, at $T/T_0 = 0.54$ and 0.61. The error bars in η and r_0 denote standard fit errors, while the error bars in temperature are statistical errors.

$T_{c,\mathrm{q2D}}/T_0 = 0.74$ [48], which is defined as the temperature at which the superfluid appears at the center of the cloud. The result of $T_{c,\mathrm{center}}$ also agrees with the quasicondensation temperature $T_{\mathrm{qc}}/T_0 \sim 0.7$. Similarly, at T_c, we observe the phase-space density (PSD) $\mathcal{D} = n\lambda^2$ at the trap center $\mathcal{D}_c = 15(2)$, where $\lambda = h/\sqrt{2\pi m k_B T}$ is the thermal de Broglie wavelength. In the limit of small regions of interest, we expect $\mathcal{D}_{c,\mathrm{center}} = 9(2)$, which is close to the theoretical prediction $\mathcal{D}_c = \ln(380/\tilde{g}) = 8.5$ [49].

In Fig. 3(b), we show the experimentally determined η and the simulation results for various temperatures across the transition, which are in good agreement. According to BKT theory, $\eta(T)$ scales approximately linearly in the superfluid phase [2,50]. Indeed, our measurement of $\eta(T)$ follows linear dependence for $T \lesssim T_c$, where the system is in the superfluid regime. However, above T_c, $\eta(T)$ deviates from the linear behavior and increases more rapidly.

At T_c, the algebraic exponent is $\eta_c \equiv \eta(T_c) = 0.17(3)$, which is below the universal value in the thermodynamic limit $\eta_{\mathrm{BKT}} = 0.25$. For a finite-size system, the transition manifests itself as a smooth crossover, for which the critical exponent displays a smaller value which scales with the system size as $\eta_c(L) = \eta_{\mathrm{BKT}}/(1 + 0.5/[\ln(L) + C])$, where L is the linear dimension of the system and C is a nonuniversal constant of order unity [51]. For our trapped system, this expression gives $\eta_c(L) \sim 0.21$ using $L \sim R/\xi \sim 30$, where $R \sim 30$ μm is the TF diameter and $\xi \sim 1$ μm is the healing length. The value of η_c is unaffected by the change in the region of interest [29].

In Fig. 3(c), we show the correlation length $r_0(T)$ and the temperature-dependent TF diameter. Since r_0 cannot exceed the system size, the value of r_0 is bounded by the TF diameter. The experimentally determined values of r_0 reach this upper bound for $T \lesssim T_c$ in the superfluid phase. When the system crosses T_c, r_0 becomes smaller than the TF diameter. We note that up to 15% systematic error in r_0 is expected from the limitations of our imaging system in the thermal regime [29]. In Fig. 3(c) we present the simulation results for $r_0(T)$ and the TF diameter, which show consistent behavior in agreement with the measurements.

The BKT transition is driven by thermal vortex unbinding, which suppresses the quasi-long-range order above the critical temperature. This underlying mechanism is detected via matter-wave interferometry, where vortices are observed as sharp dislocations in the interference patterns [8]. This enables us to determine the local vortex density using our selective imaging method [21,29]. In Fig. 4(a), we show examples of matter-wave interference patterns obtained from two independent measurements at $T/T_0 = 0.52$ and 0.55. The sharp phase dislocations are indicated by red vertical lines, which we count as vortices. We obtain local vortex density $n_v(x)$ by averaging the vortex number over many images at the location x [29]. In Fig. 4(b), we show the probability to detect a vortex P_v, averaged over the TF region; there is a sharp increase in P_v at a certain temperature. We determine this vortex proliferation temperature, $T_v/T_0 = 0.52(1)$, from the discontinuity of the slope in a piecewise linear fit.

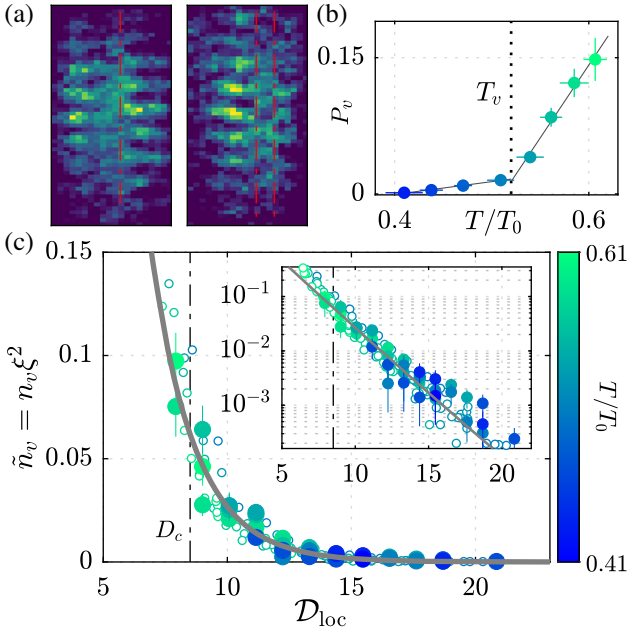

FIG. 4. Vortex proliferation in 2D Bose gases. (a) Typical interference patterns with phase dislocations (indicated by red vertical lines), which we count as vortices. (b) Probability to detect a vortex P_v as a function of T/T_0. The vertical dotted line is the vortex proliferation temperature T_v, which is determined using a piecewise linear fit (continuous lines). The error bars for P_v are the statistical uncertainty, given by the square root of the numbers of detected vortices. (c) The rescaled local vortex density $\tilde{n}_v(x) = n_v(x)\xi(x)^2$ plotted against the local PSD $\mathcal{D}_{\mathrm{loc}} = n(x)\lambda(T)^2$, where $n(x)$ is the local 2D density at location x. The measurements (filled circles) and the simulations (open circles) cover a range of temperatures between $T/T_0 = 0.41$ and 0.61 and experimental datasets with eight different temperatures contribute to the plot. The solid line is the exponential fit to the experimental data; see text. The vertical dash-dotted line is the predicted critical PSD [49]. The inset shows the same results on a log-linear scale to highlight the exponential scaling across the BKT transition. Error bars are statistical.

Weakly interacting 2D Bose gases possess a symmetry which gives rise to the scale-invariant description across the BKT critical point [16,49,52]. In an inhomogeneous system, local observables can be mapped to a scale-invariant description within LDA, using an appropriate rescaling of the quantities [16]. In Fig. 4(c) we plot the rescaled local vortex density $\tilde{n}_v = n_v(x)\xi(x)^2$ against the local PSD $\mathcal{D}_{\mathrm{loc}} = n(x)\lambda^2$, where $n(x)$ is the local 2D density at the location x and $\xi(x) = 1/\sqrt{n_{\mathrm{qc}}(x)\tilde{g}}$ is the local healing length calculated using the quasicondensate density n_{qc} [29]. The healing length characterizes the length scale of a vortex core with its area $\sim\xi^2$, such that $\tilde{n}_v$ quantifies the dimensionless vortex core density.

The measurements for different temperatures collapse on to a common exponential (continuous line), as clearly shown in the inset. This is a direct demonstration of scale invariance of vortex density near the BKT transition. The vortex density grows exponentially at low $\mathcal{D}_{\mathrm{loc}}$, indicating crossover to the thermal phase. We fit the measured local vortex density with the function $Ae^{-\gamma\mathcal{D}_{\mathrm{loc}}}$, where A and γ are the fit parameters. This choice of exponential scaling is motivated by Ref. [53]. From the fit, we obtain $\gamma_{\mathrm{Exp}} = 0.56(5)$ and $A_{\mathrm{Exp}} = 7(2)$. In Fig. 4(c) we also present the simulation result of the vortex density [29], which shows scale-invariant behavior that agrees with the measurements with $\gamma_{\mathrm{MC}} = 0.52(5)$.

In conclusion, we have measured the local phase fluctuations of 2D Bose gases via matter-wave interferometry and supported the measurements by Monte Carlo simulations. Our measurements of the phase correlation function and the vortex density provide a comprehensive understanding of the BKT transition in 2D Bose gases. We identified the critical point by the sudden change in the functional form of correlation function. We have mapped out the temperature dependence of the algebraic exponent and determined $\eta_c = 0.17(3)$, as expected for a finite-size system. The local vortex density shows a scale-invariant behavior across the transition.

The experimental technique presented in this Letter can be used to probe nonequilibrium dynamics across the BKT transition [54–56]. Furthermore, the pair of 2D gases in two trap minima can be coupled via quantum tunneling, to investigate the coupled bilayer XY model [57] and Josephson dynamics in low-dimensional quantum gases [58,59].

We acknowledge discussions with Junichi Okamoto, Beilei Zhu, and Zoran Hadzibabic. This work was supported by the EPSRC Grant Reference EP/S013105/1. S. S. acknowledges the Murata scholarship foundation, Ezoe Foundation, Daishin Foundation, and St Hilda's College for financial support. D. G., A. B., A. J. B., and K. L. thank the EPSRC for doctoral training funding. L. M. acknowledges funding by the Deutsche Forschungsgemeinschaft (DFG) in the framework of SFB 925—project ID 170620586 and the Excellence Cluster "Advanced Imaging of Matter"—EXC 2056—project ID 390715994. V. P. S. acknowledges funding by the Cluster of Excellence "QuantumFrontiers"—EXC 2123—project ID 390837967.

*shinichi.sunami@physics.ox.ac.uk

[1] V. Berezinskii, Destruction of long-range order in one-dimensional and two-dimensional systems possessing a continuous symmetry group. II. Quantum systems, Sov. Phys. JETP **34**, 610 (1972).

[2] J. M. Kosterlitz and D. J. Thouless, Ordering, metastability and phase transitions in two-dimensional systems, J. Phys. C **6**, 1181 (1973).

[3] N. D. Mermin and H. Wagner, Absence of Ferromagnetism or Antiferromagnetism in One- or Two-Dimensional Isotropic Heisenberg Models, Phys. Rev. Lett. **17**, 1307 (1966).

[4] P. C. Hohenberg, Existence of long-range order in one and two dimensions, Phys. Rev. **158**, 383 (1967).

[5] D. J. Bishop and J. D. Reppy, Study of the Superfluid Transition in Two-Dimensional ^{4}He Films, Phys. Rev. Lett. **40**, 1727 (1978).

[6] K. Epstein, A. M. Goldman, and A. M. Kadin, Vortex-Antivortex Pair Dissociation in Two-Dimensional Superconductors, Phys. Rev. Lett. **47**, 534 (1981).

[7] D. J. Resnick, J. C. Garland, J. T. Boyd, S. Shoemaker, and R. S. Newrock, Kosterlitz-Thouless Transition in Proximity-Coupled Superconducting Arrays, Phys. Rev. Lett. **47**, 1542 (1981).

[8] Z. Hadzibabic, P. Krüger, M. Cheneau, B. Battelier, and J. Dalibard, Berezinskii-Kosterlitz-Thouless crossover in a trapped atomic gas, Nature (London) **441**, 1118 (2006).

[9] D. Caputo, D. Ballarini, G. Dagvadorj, C. S. Munõz, M. De Giorgi, L. Dominici, K. West, L. N. Pfeiffer, G. Gigli, F. P. Laussy, M. H. Szymanska, and D. Sanvitto, Topological order and thermal equilibrium in polariton condensates, Nat. Mater. **17**, 145 (2018).

[10] R. Desbuquois, L. Chomaz, T. Yefsah, J. Léonard, J. Beugnon, C. Weitenberg, and J. Dalibard, Superfluid behaviour of a two-dimensional Bose gas, Nat. Phys. **8**, 645 (2012).

[11] N. Luick, L. Sobirey, M. Bohlen, V. P. Singh, L. Mathey, T. Lompe, and H. Moritz, An ideal Josephson junction in an ultracold two-dimensional Fermi gas, Science **369**, 89 (2020).

[12] L. Sobirey, N. Luick, M. Bohlen, H. Biss, H. Moritz, and T. Lompe, Observation of superfluidity in a strongly correlated two-dimensional Fermi gas, Science **372**, 844 (2021).

[13] J. Choi, S. W. Seo, W. J. Kwon, and Y. Shin, Probing Phase Fluctuations in a 2D Degenerate Bose Gas by Free Expansion, Phys. Rev. Lett. **109**, 125301 (2012).

[14] W. J. Kwon, G. Moon, S. W. Seo, and Y. Shin, Critical velocity for vortex shedding in a Bose-Einstein condensate, Phys. Rev. A **91**, 053615 (2015).

[15] C. D. Rossi, R. Dubessy, K. Merloti, M. de Goër de Herve, T. Badr, A. Perrin, L. Longchambon, and H. Perrin, Probing superfluidity in a quasi two-dimensional Bose gas through its local dynamics, New J. Phys. **18**, 062001 (2016).

[16] C. L. Hung, X. Zhang, N. Gemelke, and C. Chin, Observation of scale invariance and universality in two-dimensional Bose gases, Nature (London) **470**, 236 (2011).

[17] J. Choi, S. W. Seo, and Y. Shin, Observation of Thermally Activated Vortex Pairs in a Quasi-2D Bose Gas, Phys. Rev. Lett. **110**, 175302 (2013).

[18] P. A. Murthy, I. Boettcher, L. Bayha, M. Holzmann, D. Kedar, M. Neidig, M. G. Ries, A. N. Wenz, G. Zürn, and S. Jochim, Observation of the Berezinskii-Kosterlitz-Thouless Phase Transition in an Ultracold Fermi Gas, Phys. Rev. Lett. **115**, 010401 (2015).

[19] R. J. Fletcher, M. Robert-de Saint-Vincent, J. Man, N. Navon, R. P. Smith, K. G. H. Viebahn, and Z. Hadzibabic, Connecting Berezinskii-Kosterlitz-Thouless and BEC Phase Transitions by Tuning Interactions in a Trapped Gas, Phys. Rev. Lett. **114**, 255302 (2015).

[20] I. Boettcher and M. Holzmann, Quasi-long-range order in trapped two-dimensional Bose gases, Phys. Rev. A **94**, 011602(R) (2016).
[21] A. J. Barker, S. Sunami, D. Garrick, A. Beregi, K. Luksch, E. Bentine, and C. J. Foot, Coherent splitting of two-dimensional Bose gases in magnetic potentials, New J. Phys. **22**, 103040 (2020).
[22] T. L. Harte, E. Bentine, K. Luksch, A. J. Barker, D. Trypogeorgos, B. Yuen, and C. J. Foot, Ultracold atoms in multiple radio-frequency dressed adiabatic potentials, Phys. Rev. A **97**, 013616 (2018).
[23] K. Merloti, R. Dubessy, L. Longchambon, A. Perrin, P. E. Pottie, V. Lorent, and H. Perrin, A two-dimensional quantum gas in a magnetic trap, New J. Phys. **15**, 033007 (2013).
[24] G. Hechenblaikner, J. M. Krueger, and C. J. Foot, Properties of quasi-two-dimensional condensates in highly anisotropic traps, Phys. Rev. A **71**, 013604 (2005).
[25] P. Cladé, C. Ryu, A. Ramanathan, K. Helmerson, and W. D. Phillips, Observation of a 2D Bose Gas: From Thermal to Quasicondensate to Superfluid, Phys. Rev. Lett. **102**, 170401 (2009).
[26] A. Posazhennikova, Colloquium: Weakly interacting, dilute Bose gases in 2D, Rev. Mod. Phys. **78**, 1111 (2006).
[27] N. Prokof'ev and B. Svistunov, Two-dimensional weakly interacting Bose gas in the fluctuation region, Phys. Rev. A **66**, 043608 (2002).
[28] N. J. van Druten and W. Ketterle, Two-Step Condensation of the Ideal Bose Gas in Highly Anisotropic Traps, Phys. Rev. Lett. **79**, 549 (1997).
[29] See Supplemental Material at http://link.aps.org/supplemental/10.1103/PhysRevLett.128.250402 for more details, which includes Refs. [30–46].
[30] C. Mora and Y. Castin, Extension of Bogoliubov theory to quasicondensates, Phys. Rev. A **67**, 053615 (2003).
[31] V. P. Singh, C. Weitenberg, J. Dalibard, and L. Mathey, Superfluidity and relaxation dynamics of a laser-stirred two-dimensional Bose gas, Phys. Rev. A **95**, 043631 (2017).
[32] V. P. Singh, N. Luick, L. Sobirey, and L. Mathey, Josephson junction dynamics in a two-dimensional ultracold Bose gas, Phys. Rev. Research **2**, 033298 (2020).
[33] V. P. Singh and L. Mathey, Collective modes and superfluidity of a two-dimensional ultracold Bose gas, Phys. Rev. Research **3**, 023112 (2021).
[34] E. Bentine, T. L. Harte, K. Luksch, A. J. Barker, J. Mur-Petit, B. Yuen, and C. J. Foot, Species-selective confinement of atoms dressed with multiple radiofrequencies, J. Phys. B **50**, 094002 (2017).
[35] E. Bentine, A. J. Barker, K. Luksch, S. Sunami, T. L. Harte, B. Yuen, C. J. Foot, D. J. Owens, and J. M. Hutson, Inelastic collisions in radiofrequency-dressed mixtures of ultracold atoms, Phys. Rev. Research **2**, 033163 (2020).
[36] A. J. Barker, S. Sunami, D. Garrick, A. Beregi, K. Luksch, E. Bentine, and C. J. Foot, Realising a species-selective double well with multiple-radiofrequency-dressed potentials, J. Phys. B **53**, 155001 (2020).
[37] M. Gildemeister, B. E. Sherlock, and C. J. Foot, Techniques to cool and rotate Bose-Einstein condensates in time-averaged adiabatic potentials, Phys. Rev. A **85**, 053401 (2012).
[38] R. P. Smith, R. L. D. Campbell, N. Tammuz, and Z. Hadzibabic, Effects of Interactions on the Critical Temperature of a Trapped Bose Gas, Phys. Rev. Lett. **106**, 250403 (2011).
[39] C. F. Ockeloen, A. F. Tauschinsky, R. J. C. Spreeuw, and S. Whitlock, Detection of small atom numbers through image processing, Phys. Rev. A **82**, 061606(R) (2010).
[40] Z. Hadzibabic, P. Krüger, M. Cheneau, S. P. Rath, and J. Dalibard, The trapped two-dimensional Bose gas: From Bose-Einstein condensation to Berezinskii-Kosterlitz-Thouless physics, New J. Phys. **10**, 045006 (2008).
[41] Z. Hadzibabic and J. Dalibard, Two-dimensional Bose fluids: An atomic physics perspective, Riv. Nuovo Cimento **6**, 0 (2011).
[42] I. G. Hughes and T. Hase, *Measurements and Their Uncertainties* (Oxford University Press, Oxford, 2010).
[43] M. Holzmann, M. Chevallier, and W. Krauth, Universal correlations and coherence in quasi-two-dimensional trapped Bose gases, Phys. Rev. A **81**, 043622 (2010).
[44] C. W. Gardiner, *Stochastic Methods*, 4th ed., Springer Series in Synergetics (Springer-Verlag, Berlin, 2009), Vol. 13.
[45] H.-P. Stimming, N. J. Mauser, J. Schmiedmayer, and I. E. Mazets, Fluctuations and Stochastic Processes in One-Dimensional Many-Body Quantum Systems, Phys. Rev. Lett. **105**, 015301 (2010).
[46] T. Langen, M. Gring, M. Kuhnert, B. Rauer, R. Geiger, D. A. Smith, I. E. Mazets, and J. Schmiedmayer, Prethermalization in one-dimensional Bose gases: Description by a stochastic Ornstein-Uhlenbeck process, Eur. Phys. J. Special Topics **217**, 43 (2013).
[47] C. J. Pethick and H. Smith, *Bose-Einstein Condensation in Dilute Gases* (Cambridge University Press, Cambridge, England, 2008).
[48] M. Holzmann, M. Chevallier, and W. Krauth, Semiclassical theory of the quasi–two-dimensional trapped Bose gas, Eur. Phys. Lett. **82**, 30001 (2008).
[49] N. Prokof'ev, O. Ruebenacker, and B. Svistunov, Critical Point of a Weakly Interacting Two-Dimensional Bose Gas, Phys. Rev. Lett. **87**, 270402 (2001).
[50] D. R. Nelson and J. M. Kosterlitz, Universal Jump in the Superfluid Density of Two-Dimensional Superfluids, Phys. Rev. Lett. **39**, 1201 (1977).
[51] H. Weber and P. Minnhagen, Monte Carlo determination of the critical temperature for the two-dimensional XY model, Phys. Rev. B **37**, 5986(R) (1988).
[52] L. P. Pitaevskii and A. Rosch, Breathing modes and hidden symmetry of trapped atoms in two dimensions, Phys. Rev. A **55**, R853 (1997).
[53] I. Maccari, N. Defenu, L. Benfatto, C. Castellani, and T. Enss, Interplay of spin waves and vortices in the two-dimensional XY model at small vortex-core energy, Phys. Rev. B **102**, 104505 (2020).
[54] L. Mathey and A. Polkovnikov, Light cone dynamics and reverse Kibble-Zurek mechanism in two-dimensional superfluids following a quantum quench, Phys. Rev. A **81**, 033605 (2010).
[55] L. Mathey, K. J. Günter, J. Dalibard, and A. Polkovnikov, Dynamic Kosterlitz-Thouless transition in two-dimensional Bose mixtures of ultracold atoms, Phys. Rev. A **95**, 053630 (2017).

[56] J. Schole, B. Nowak, and T. Gasenzer, Critical dynamics of a two-dimensional superfluid near a nonthermal fixed point, Phys. Rev. A **86**, 013624 (2012).

[57] L. Mathey, A. Polkovnikov, and A. H. C. Neto, Phase-Locking Transition of Coupled Low-Dimensional Superfluids, Eur. Phys. Lett. **81**, 10008 (2007).

[58] Y. D. van Nieuwkerk and F. H. L. Essler, Self-consistent time-dependent harmonic approximation for the Sine-Gordon model out of equilibrium, J. Stat. Mech. (2019) 084012.

[59] B. Zhu, V. P. Singh, J. Okamoto, and L. Mathey, Dynamical control of the conductivity of an atomic Josephson junction, Phys. Rev. Research **3**, 013111 (2021).